



HAL
open science

Probing the acid sites of zeolites with pyridine: quantitative AGIR measurements of the molar absorption coefficients

Vladimir Zholobenko, Cátia Freitas, Martin Jendrlin, Philippe Bazin, Arnaud Travert, Frederic Thibault-Starzyk

► To cite this version:

Vladimir Zholobenko, Cátia Freitas, Martin Jendrlin, Philippe Bazin, Arnaud Travert, et al.. Probing the acid sites of zeolites with pyridine: quantitative AGIR measurements of the molar absorption coefficients. *Journal of Catalysis*, 2020, 385, pp.52–60. 10.1016/j.jcat.2020.03.003 . hal-02500425

HAL Id: hal-02500425

<https://hal.science/hal-02500425v1>

Submitted on 5 Mar 2020

HAL is a multi-disciplinary open access archive for the deposit and dissemination of scientific research documents, whether they are published or not. The documents may come from teaching and research institutions in France or abroad, or from public or private research centers.

L'archive ouverte pluridisciplinaire **HAL**, est destinée au dépôt et à la diffusion de documents scientifiques de niveau recherche, publiés ou non, émanant des établissements d'enseignement et de recherche français ou étrangers, des laboratoires publics ou privés.

1 **Probing the acid sites of zeolites with pyridine: quantitative AGIR**
2 **measurements of the molar absorption coefficients**

3
4 Vladimir Zholobenko ^{a,b} *, Cátia Freitas ^b, Martin Jendrlin ^b, Philippe Bazin ^a, Arnaud Travert ^a,
5 Frederic Thibault-Starzyk ^a

6
7 ^a Normandie Univ, ENSICAEN, CNRS, Laboratoire Catalyse et Spectrochimie, France

8 ^b School of Chemical and Physical Sciences, Keele University, United Kingdom

9
10 **Abstract**

11 This study presents a detailed methodology, which combines high-precision thermogravimetry and
12 FTIR spectroscopy, aiming to establish the most accurate and reliable means of measuring the
13 molar absorption coefficients of adsorbed species. As the integrated molar absorption coefficients
14 of Py complexes with Brønsted and Lewis acid sites, $\epsilon(\text{Py-B})$ and $\epsilon(\text{Py-L})$, are determined and the
15 validity of the Beer-Lambert-Bouguer law for IR characterisation of solid acids is demonstrated,
16 this work is setting a benchmark for the quantitative acidity measurements in zeolites and related
17 materials. The following values of $\epsilon(\text{Py-B})$ have been obtained at 150°C (band at $\sim 1545 \text{ cm}^{-1}$):
18 $1.09 \pm 0.08 \text{ cm } \mu\text{mol}^{-1}$ for ZSM-5; $1.12 \pm 0.16 \text{ cm } \mu\text{mol}^{-1}$ for BEA; $1.29 \pm 0.04 \text{ cm } \mu\text{mol}^{-1}$ for MOR
19 and $1.54 \pm 0.15 \text{ cm } \mu\text{mol}^{-1}$ for FAU. The value of $\epsilon(\text{Py-L})$ (band at $\sim 1455 \text{ cm}^{-1}$, which refers to
20 different cations) measured at the same temperature is $1.71 \pm 0.1 \text{ cm } \mu\text{mol}^{-1}$. Values of $\epsilon(\text{Py-B})$
21 depend on the zeolite structure, in contrast to that for $\epsilon(\text{Py-L})$. Clear correlations are presented
22 between the temperature of the FTIR measurements and ϵ values for Py complexes and other
23 species, which decrease by $\sim 10\%$ as the temperature increases by 100°C. In addition, the effects of
24 key experimental procedures, instrumentation design and sample preparation are established and
25 quantified.

26
27
28 **Key words:** zeolites; acid sites; FTIR; pyridine; molar absorption coefficients

29
30 * Corresponding author: v.l.zholobenko@keele.ac.uk

31

32 1. Introduction

33 Zeolites, particularly crystalline aluminosilicates, are essential for a host of major industrial
34 processes. They are utilised as molecular sieves, for nuclear waste clean-up, as water softeners in
35 washing powders, as vital catalysts in oil refining and petrochemical industries for the production of
36 petrol and diesel, olefins and simple aromatic compounds, polymers and plastics, etc. The
37 successful application of these materials in catalysis is associated with their microporous structure
38 and highly effective acid sites. Hence, characterisation of the acidic properties of zeolites is of
39 significant fundamental and practical importance. Over several decades, pyridine (Py) has been the
40 most frequently utilised infrared probe molecule for the characterisation of active sites in solid acids
41 [see review 1 and references therein]. Indeed, (i) Py complexes with acid sites can be easily
42 discriminated in the spectra, thus Brønsted and Lewis acid sites (BAS and LAS) can be evaluated;
43 (ii) Py is a rather stable molecule at a wide range of characterisation conditions, allowing for
44 instance, high-temperature experiments, such as TPD; (iii) Py and its derivatives can be used to
45 examine the accessibility of the acid sites in a variety of zeolite structures. In addition, FTIR spectra
46 of adsorbed Py can be used for quantitative measurements of the number of acid sites present in a
47 solid catalyst via the application of the Beer-Lambert law (this should be referred to as the Beer-
48 Lambert-Bouguer law to acknowledge the original contribution by Pierre Bouguer). A wide range
49 of molar absorption coefficient values can be found in the literature (Table 1) for Py adsorbed on
50 BAS and LAS, $\epsilon(\text{Py-B})$ and $\epsilon(\text{Py-L})$. However, there are significant differences among the data
51 published by different researchers: the ϵ values vary by six orders of magnitude, the $\epsilon(\text{Py-B})/\epsilon(\text{Py-L})$
52 ratios are between 0.47 and 8.8, and different units of ϵ are reported (Table 1), suggesting that
53 such variations may be associated with significant errors [1]. Furthermore, the details of
54 experimental procedures, which differ a great deal, and of the data analysis are frequently unclear or
55 incomplete. In addition, the application of the classic Beer-Lambert-Bouguer law to the FTIR
56 characterisation of solid catalysts is challenging, and the accuracy of quantitative data reported in
57 the literature may be limited by the equipment available and the methodology utilised in such
58 research. Indeed, the physical parameters and properties of the sample (its thickness, pressure used
59 to prepare the disc, particle size, etc.) and the experimental design (spectral resolution, temperature
60 of the FTIR measurements, using a vacuum system or a gas flow) may have a large influence on the
61 ϵ values obtained [2]. It should be noted that for other probe molecules there are quantitative data in
62 the literature, including the calculation of ϵ values for ammonia, quinoline, acetonitrile and
63 substituted pyridines [1,3-8], but, these are not discussed in the present work.

64

Table 1. Molar absorption coefficients (ϵ) values for Py adsorbed on BAS and LAS reported in the literature.

Material	$\epsilon(\text{Py-B})$	Units	$\epsilon(\text{Py-L})$	Units	$\frac{\epsilon(\text{Py-B})}{\epsilon(\text{Py-L})}$	Resolution, cm^{-1}	Temperature, $^{\circ}\text{C}$	Year	Ref
Silica-alumina	-	-	-	-	$8.8 \pm 15\%$	2 or 4	-	1964	[9]
Silica-alumina	-	-	-	-	6.0 ± 9	-	-	1966	[10]
NH ₄ Y	3.03 ± 0.13	$\text{cm } \mu\text{mol}^{-1}$	3.26 ± 0.13	$\text{cm } \mu\text{mol}^{-1}$	0.93	-	150	1967	[11]
MOR	-	-	-	-	2.61	-	-	1968	[12]
MOR	-	-	-	-	1.54	4	-	1971	[13]
NaY	0.059 ± 0.004	$\mu\text{mol cm}^{-2}$	-	-	-	-	150	1980	[14]
NaHY	0.059 ± 0.004	$\text{cm}^2 \mu\text{mol}^{-1}$	0.084 ± 0.003	$\text{cm}^2 \mu\text{mol}^{-1}$	0.70	-	-	1981	[15]
ZSM-5	1.3×10^{-6}	$\text{cm } \mu\text{mol}^{-1}$	1.5×10^{-6}	$\text{cm } \mu\text{mol}^{-1}$	0.87	-	150	1986	[16]
Al ₂ O ₃ , Y	0.73	$\text{cm } \mu\text{mol}^{-1}$	1.11	$\text{cm } \mu\text{mol}^{-1}$	0.66	2	200	1992	[17]
MOR, ZSM-5, Y	1.67 ± 0.12	$\text{cm } \mu\text{mol}^{-1}$	2.22 ± 0.21	$\text{cm } \mu\text{mol}$	0.75	1	150 and 350	1993	[18]
BEA	1.3×10^{-6}	$\text{cm } \mu\text{mol}^{-1}$	1.5×10^{-6}	$\text{cm } \mu\text{mol}^{-1}$	0.87	-	30	1994	[19]
HY	1.8 ± 0.1	$\text{cm } \mu\text{mol}^{-1}$	1.5	$\text{cm } \mu\text{mol}^{-1}$	1.2	-	-	1994	[20]
Y	1.1	$\text{cm } \mu\text{mol}^{-1}$	-	-	-	2	30	1995	[21]
EMT	1.6	$\text{cm } \mu\text{mol}^{-1}$	-	-	-	-	30	1995	[22]
MOR	1.8	$\text{cm } \mu\text{mol}^{-1}$	-	-	-	2	30	1995	[22]
MOR, Y	0.078 ± 0.004	$\text{cm}^2 \mu\text{mol}$	0.269 ± 0.01	$\text{cm}^2 \mu\text{mol}$	0.29	-	145	1996	[23]
MOR, Al ₂ O ₃	1.13	$\text{cm } \mu\text{mol}^{-1}$	1.28	$\text{cm } \mu\text{mol}^{-1}$	0.88	-	-	1997	[24]
Y	0.085 ± 0.005	$\text{cm}^2 \mu\text{mol}$	-	-	-	-	145	1997	[25]

MAZ	1.13	cm μmol^{-1}	1.28	cm μmol^{-1}	0.88	-	-	1998	[26]
MCM-41	1.47	cm μmol^{-1}	1.98	cm μmol^{-1}	0.74	-	150	1999	[27]
BEA, MOR, Y, Silica-alumina	0.73±0.04	cm μmol^{-1}	0.64±0.04	cm μmol^{-1}	1.14	2	150	1999	[28]
Y	1.36±0.03	cm μmol^{-1}	-	-	-	4	200	2004	[29]
HMCM-41, Al₂O₃	0.070	cm μmol^{-1}	0.100	cm μmol^{-1}	0.70	2	150	2005	[30]
BEA, VBEA	0.070	cm μmol^{-1}	0.100	cm μmol^{-1}	0.70	2	150	2006	[31]
MCM-48, MCM-68	0.078	cm μmol^{-1}	0.165	cm μmol^{-1}	0.47	2	170	2010	[32]
Silica-alumina	0.57	cm μmol^{-1}	1.5	cm μmol^{-1}	0.38	-	-	2010	[33]
SBA-15	1.67±0.12	cm μmol	2.22±0.21	cm μmol	0.75	4	30	2010	[34]
Silica-alumina	1.67±0.12	cm μmol	2.22±0.21	cm μmol	0.75	4	150	2012	[35]
HY	1.95±0.13	cm μmol^{-1}	1.45±0.10	cm μmol^{-1}	1.34	2	150	2016	[36]
SnBEA	-	-	1.42±0.30	cm μmol^{-1}	1.37				
SAPO-34	0.06	cm ² μmol^{-1}	-	-	-	4	-	2017	[37]
ZSM-5	0.07	cm ² μmol^{-1}	0.10	cm ² μmol^{-1}	0.70	2	170	2017	[38]
BEA	1.98±0.16		2.53±0.38		0.78				
ZSM-5	2.98±0.49	mmol/g _{cat} /area	~2.2	mmol/g _{cat} /area	1.35	4	30	2018	[39]
Y	2.55±0.28		2.27±0.41		1.12				

1 Significant advances in the design of new instrumentation for the accurate quantitative
2 analysis of the FTIR spectra have been made in the last few years [7,29,40], such as the
3 combination of high-precision thermogravimetry and FTIR spectroscopy (AGIR, combining
4 gravimetric analysis and IR). This technique, in which a microbalance is integrated with an FTIR in
5 situ cell within a single set-up, allows simultaneous monitoring of the weight changes of the sample
6 along with its IR spectra during adsorption or desorption of probe molecules, and consequently,
7 highly accurate quantitative data, e.g. the molar absorption coefficient values, can be obtained
8 directly, as demonstrated in [41-43]. The aim of this work is to carry out quantitative analysis of the
9 number of acid sites in different zeolites, to determine the value of the integrated molar absorption
10 coefficients of Py adsorbed on Brønsted and Lewis acid sites and to examine the role of
11 experimental conditions that are essential for the reliable characterisation of the acidic properties of
12 zeolite-based catalysts. This study also examines the validity of the Beer-Lambert-Bouguer law in
13 solid materials. The $\epsilon(\text{Py-B})$ and $\epsilon(\text{Py-L})$ values have been determined using the AGIR technique,
14 which, we believe, is the most accurate and reliable method of measuring the molar absorption
15 (extinction) coefficients of adsorbed species. Overall, the optimisation of the experimental
16 procedures is imperative for the successful quantitative evaluation of different types of acid sites in
17 zeolitic materials. With the new level of instrumentation available now, this work sets a benchmark
18 for the quantitative acidity measurements in zeolites and related materials.

19

20 **2. Experimental**

21 *Materials.* Ammonium forms of zeolites BEA-12 (CP814E, Zeolyst International,
22 Si/Al=12.5), BEA-19 (CP814C, Zeolyst International, Si/Al=19) ZSM-5-40 (MFI structure type,
23 CBV8014, Zeolyst International, Si/Al=40), ZSM-5-27 (MFI structure type, NIST reference
24 material RM8852, Si/Al=27 [44]), MOR-7 (Crosfield, Si/Al=7.0), MOR-10 (CBV21A, Zeolyst
25 International, Si/Al=10) FAU-C (Crosfield, Si/Al=2.6), FAU-Z (CBV300, Zeolyst International,
26 Si/Al=2.6), γ -alumina (Puralox, Sasol) and fumed silica (SiO_2 , Sigma-Aldrich, 99.8%) were either
27 used as received or calcined ex situ at 450-900°C in a muffle furnace for 5 hours. This procedure
28 allowed to obtain materials from the same type of the zeolite framework but with different
29 BAS/LAS ratios. In addition, a sample of US-Y zeolite (Crosfield, Si/Al=6) was used in this group
30 of samples. All the parent zeolites are readily available commercial samples, whose XRD patterns,
31 textural properties, SEM and TEM images, NMR and FTIR spectroscopic data can be found in the
32 literature. To account for the potential batch to batch variations and the differences in the
33 methodologies applied by various research groups, characterisation data for the samples studied in
34 this work are presented in the Appendix of the Supplementary Information section (SI).

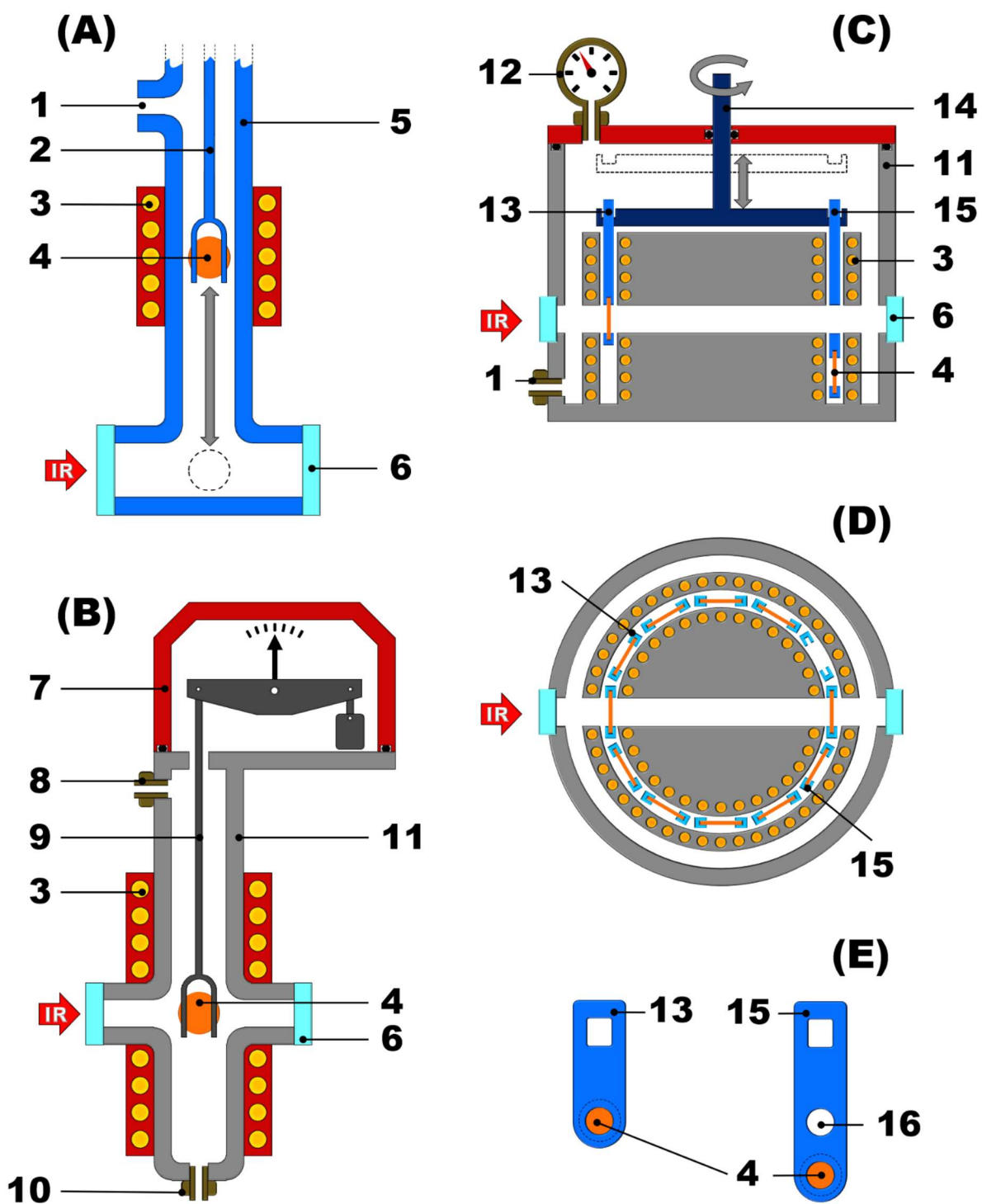
35 *In situ FTIR experiments.* An in situ IR cell was attached to a vacuum system (dynamic
36 vacuum better than 10^{-5} mbar) and the FTIR measurements were carried out using a Thermo iS10

37 FTIR spectrometer, equipped with a DTGS detector, in the range 6000-1000 cm^{-1} at a spectral
38 resolution of 1-8 cm^{-1} (typically 4 cm^{-1}) and 64 scans in transmission mode (Figures 1 and S1).
39 Prior to recording the spectra, a self-supported sample disk (1.3 cm in diameter, $S=1.3 \text{ cm}^2$; 1.5 to
40 30 mg/cm^2 , but typically 7-10 mg/cm^2) was activated in the *in situ* vacuum cell typically at 450°C
41 (ramp 1°C/min). After a period of 5 hours at the selected activation temperature, the sample was
42 cooled to the desired temperature (between 50 and 350°C) in vacuum and its IR spectrum was
43 collected. Small portions of the probe molecule, Py ($\text{C}_5\text{H}_5\text{N}$, Acros Organics, 99.5%, dried over 3A
44 molecular sieve), were admitted into the cell, usually at 150°C, until no changes in the peak
45 intensities were observed in the spectra. Physisorbed molecules were subsequently removed by
46 evacuation at 150°C. Py adsorption-desorption was carried out typically at 150-350°C. The FTIR
47 spectra were collected at different temperatures, typically between 50 and 350°C. The obtained
48 spectra were analysed, including integration, subtraction and determination of peak positions, using
49 specialised Thermo software, Omnic. The integration limits were 1565 to 1515 cm^{-1} for the Py-B
50 peak and 1465 to 1535 cm^{-1} for the Py-L peak ($\pm 3 \text{ cm}^{-1}$ depending on the nature of the sample and
51 the temperature of the FTIR measurements).

52 *CARROUCELL experiments.* The statistical CARROUCELL experiments were performed in
53 a specially designed *in situ* cell, attached to a vacuum system accommodating up to 12 samples
54 (Figure 1). 10 self-supported sample disks (1.6 cm in diameter, $S=2.0 \text{ cm}^2$; $\sim 10 \text{ mg}/\text{cm}^2$) were
55 activated under vacuum at 450°C for 5 hours (ramp 1°C/min). FTIR spectra of the samples before
56 and after Py adsorption were recorded at 30-450°C using a Thermo iS50 FTIR spectrometer
57 equipped with an MCT detector, at a spectral resolution of 4 cm^{-1} . The zeolite samples were
58 prepared by different researchers to test the “operator effect” on the quality of the data. In addition,
59 FTIR measurements for every sample were repeated using a “second round” of the CARROUCELL
60 (the time delay between the two rounds was ~ 30 minutes) to evaluate the “instrumentation effect”
61 on the data quality.

62 *AGIR experiments.* With the AGIR set-up, the mass (and therefore the number of adsorbed
63 molecules) and FTIR spectra of the sample can be measured simultaneously in real-time in a gas
64 flow system at temperatures between 30 and 500°C (Figures 1 and S2) [7]. The analyses were
65 carried out on self-supported discs ($\sim 20 \text{ mg}$, 1.6 cm in diameter, $S=2.0 \text{ cm}^2$), which were activated
66 in the IR reactor-cell at 450°C under a flow of Ar for 5 h (ramp 1°C/min). FTIR spectra of the
67 samples were recorded at 30-450°C every 300 seconds using a Thermo Nicolet 6700 spectrometer
68 equipped with an MCT detector, typically at a spectral resolution of 4 cm^{-1} (Figure S2). The mass
69 changes of the same sample were continuously monitored by a SETSYS-B Setaram microbalance
70 (the temporal resolution of ~ 10 sec and accuracy of the mass measurements better than $\pm 1 \mu\text{g}$) and
71 the gas flow composition was analysed by a Pfeiffer Omnistar GSD301 mass-spectrometer.

72



73

74 **Figure 1.** Schematics of the IR cells used in this work: (A) “classical” in situ IR cell (bottom part),
 75 (B) AGIR set-up, (C) longitudinal and (D) top (scale = 0.5) views of the CARROUCELL cell and
 76 (E) CARROUCELL sample holders. 1 - connection to the vacuum set-up, 2 - sample holder
 77 (quartz), 3 - heating element, 4 - sample disc, 5 - body of the cell (quartz), 6 - KBr window, 7 - head
 78 of the microbalance, 8 - inlet gas connection, 9 - sample holder (stainless steel), 10 - outlet gas
 79 connection, 11 - body of the cell (stainless steel), 12 - pressure gauge, 13 - small sample holder
 80 (quartz), 14 - rotating rack for 12 sample holders (in stainless steel), 15 - high sample holder
 81 (quartz), 16 - through-hole for the IR beam.

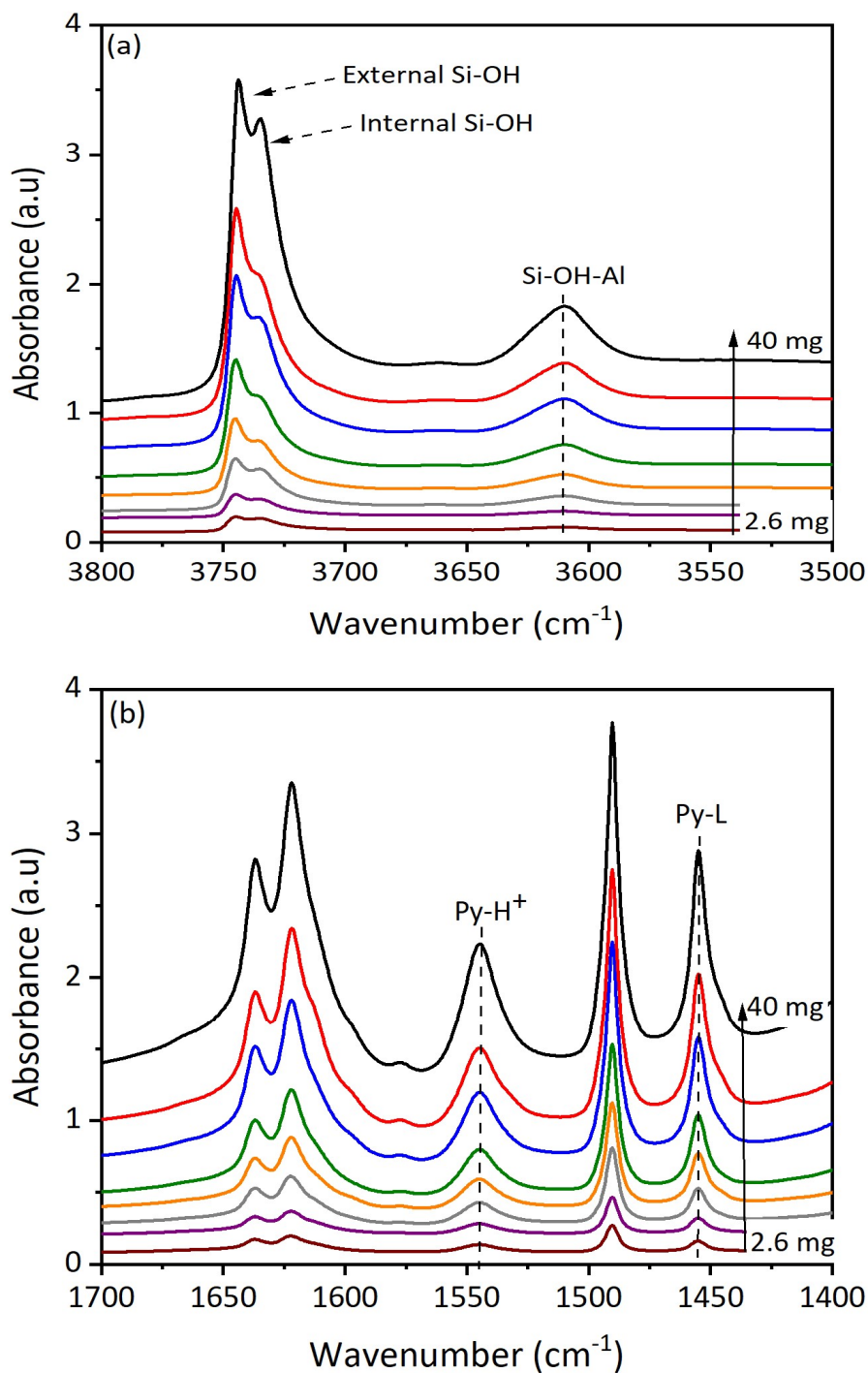
82

83 **3. Results and Discussion**

84 Preliminary work carried out to check the validity of the Beer-Lambert-Bouguer law for the
85 FTIR characterisation of zeolites and to illustrate the effects of the preparation procedure on
86 quantitative measurements is presented in SI (this includes the initial titration-style FTIR
87 measurements and a SEM examination of the self-supported IR discs, Figures S3-S6). The acid site
88 titration experiments involve admitting small doses of Py into the in situ IR cell while changes in
89 the intensity of the IR peaks are monitored. FTIR spectra of the activated BEA zeolite show major
90 peaks in the OH-region at 3745 cm^{-1} , with a shoulder at $\sim 3735\text{ cm}^{-1}$, which are attributed to the
91 external and internal Si-OH groups, and at 3610 cm^{-1} assigned to the acidic bridging Si-OH-Al
92 groups (Figure 2). The interaction of Py with the zeolite leads to a decrease in the intensity of the
93 Si-OH and Si-OH-Al bands and gives rise to the following sets of peaks: two peaks at ~ 1545 (ν_{19b})
94 and 1637 (ν_{8a}) cm^{-1} due to pyridinium ions resulting from Py protonation on Brønsted acid sites
95 (Py-B complexes, i.e. protonated Py, Py-H^+), two peaks assigned to Py coordinated to Lewis acid
96 sites (Py-L complexes) at ~ 1456 (ν_{19b}) and 1622 (ν_{8a}) cm^{-1} and overlapping signals of Py on Lewis
97 and Brønsted acid sites at ~ 1491 (ν_{19a}) cm^{-1} . In the presence of H-bonded and physisorbed Py,
98 additional peaks or shoulders are observed in the spectra, at ~ 1595 and 1580 cm^{-1} for the ν_{8a} mode,
99 as well as at ~ 1445 and 1438 cm^{-1} for ν_{19b} . The low-intensity peak, detected at 1580 cm^{-1} after the
100 removal of physisorbed Py, can be attributed to the ν_{8b} mode of Py-L complexes.

101

102



104 **Figure 2.** (a) FTIR spectra of the OH-region prior to Py adsorption and (b) difference FTIR spectra
 105 of the Py region following Py adsorption at 150°C collected on BEA-12 discs of different mass (~2-
 106 40 mg, 1.3 cm in diameter, $S=1.3 \text{ cm}^2$; spectra collected at 90°C).

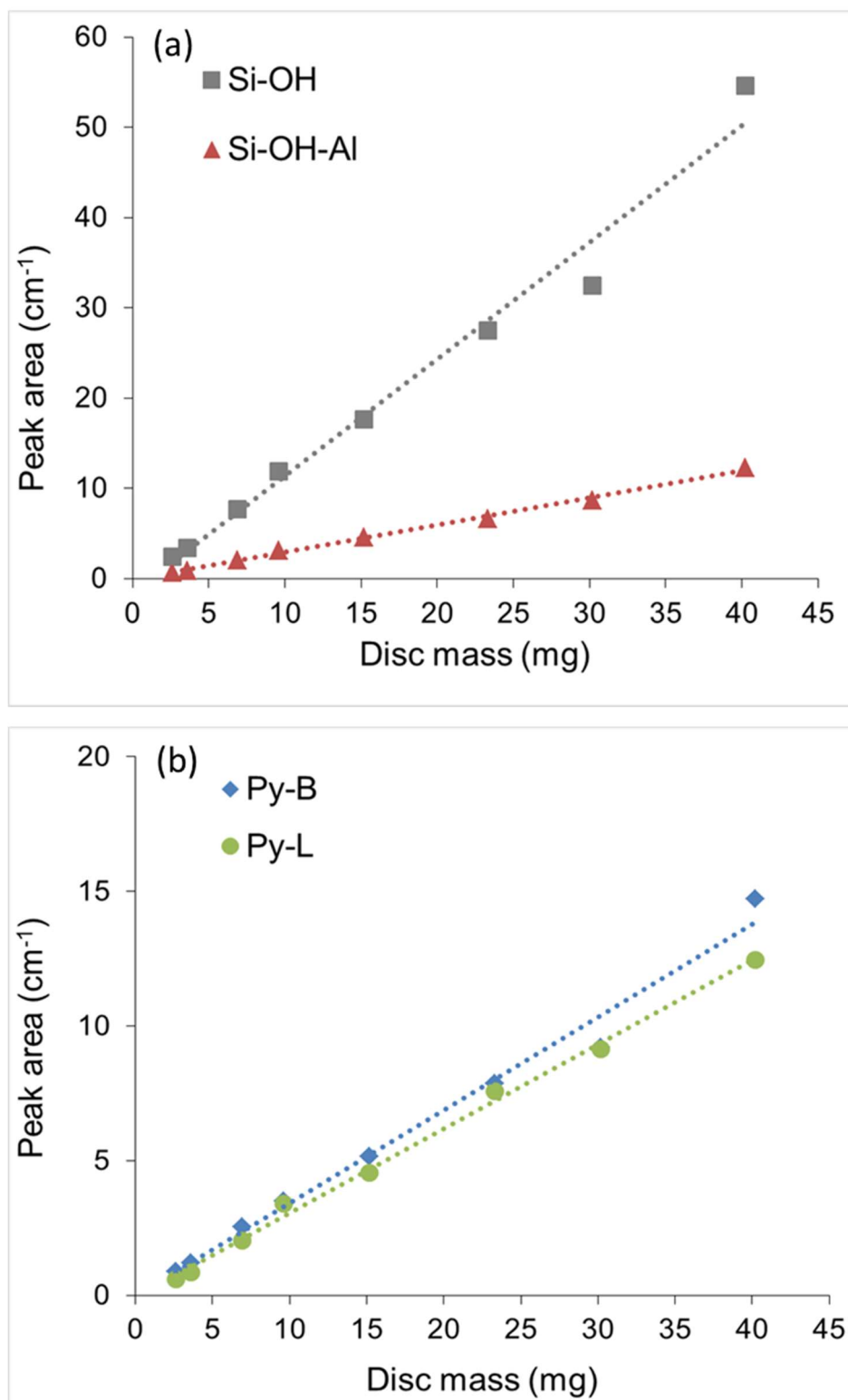
107

108 Next, the effect of the sample mass, which is used as a proxy for the effective sample
109 pathlength, on the intensity of the IR peaks has been investigated. The quantitative data obtained
110 (e.g. Figure 2) have been used to validate the Beer-Lambert-Bouguer law. The intensities of the
111 peaks of Si-OH-Al ($\sim 3610\text{ cm}^{-1}$), Si-OH ($\sim 3745\text{ cm}^{-1}$) groups, Py-B ($\sim 1545\text{ cm}^{-1}$) and Py-L (~ 1456
112 cm^{-1}) complexes increase with the sample mass (Figures 2 and 3). The data show a clear linear
113 relationship between absorbance (measured either as the peak area or peak height) and the mass of
114 the discs, demonstrating that the Beer-Lambert-Bouguer law is valid for solid materials in IR
115 spectroscopy (Figures 3 and S5), although, some noticeable deviation from it is observed for
116 samples heavier than 25 mg (i.e. $>20\text{ mg/cm}^2$; Figure S6). For practical FTIR measurements, the
117 sample size between 5 and 15 mg/cm^2 should be recommended. Our results demonstrate that the
118 sample preparation and activation procedures need to be carefully controlled in order to obtain
119 quantitative data. Although the experimental data confirm the validity of the Beer-Lambert-Bouguer
120 law for solid materials, these measurements have been performed with a BEA zeolite with low
121 scattering in the mid-IR range. For materials which strongly scatter IR radiation, the sample density
122 should be limited to $\sim 10\text{ mg/cm}^2$ to ensure both good quality and quantitative nature of the FTIR
123 measurements. It is important to note that the pressure applied while making the self-supporting
124 discs should be kept to a minimum, certainly below 0.5 tones/cm^2 , as a higher pressure can lead to
125 the incomplete sample activation (see Figure S7 and related comments) and structural degradation
126 in extreme cases.

127 The results of statistical CARROUCELL experiments carried out on five ZSM-5-40 and five
128 BEA-12 samples are presented in Figures S8-S10 and Table S1. The data demonstrate that for the in
129 situ FTIR measurements, the instrumentation errors are within $\pm 1\%$, whereas those associated with
130 the sample preparation (the “operator effect”) can be around $\pm 10\%$. The overall error can be
131 reduced to about $\pm 5\%$ by carrying out repeated measurements (5 samples in this work).

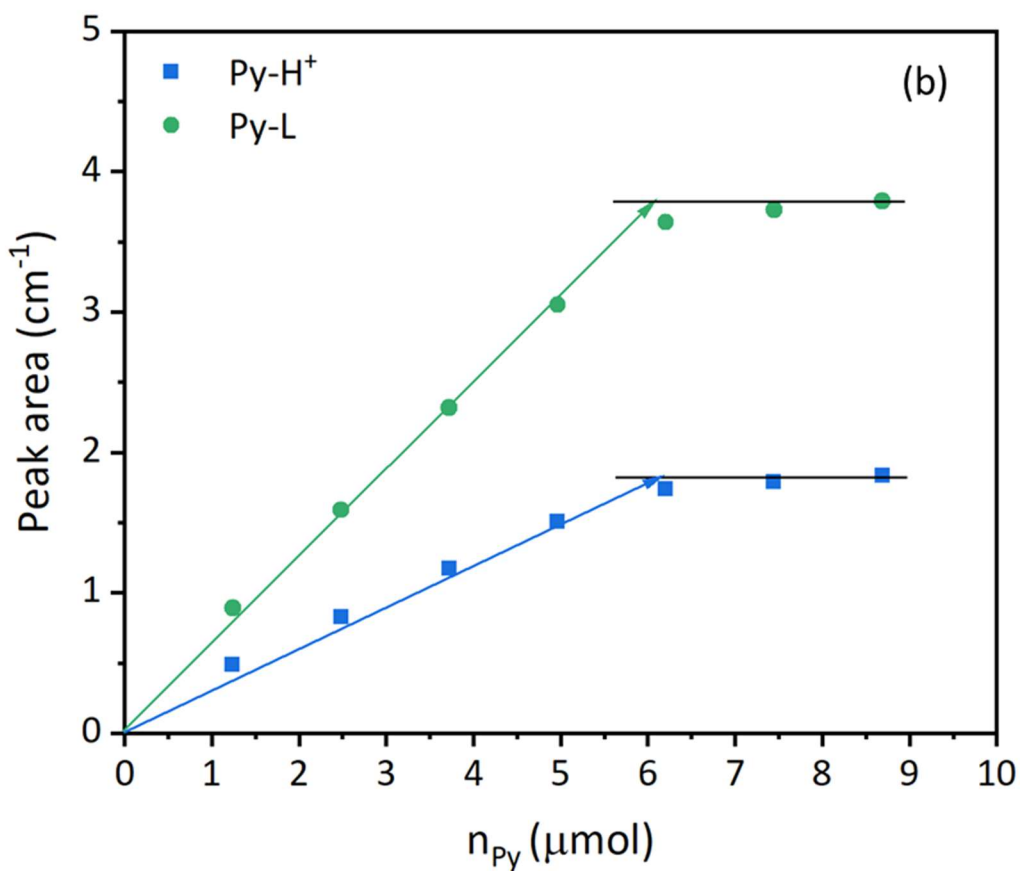
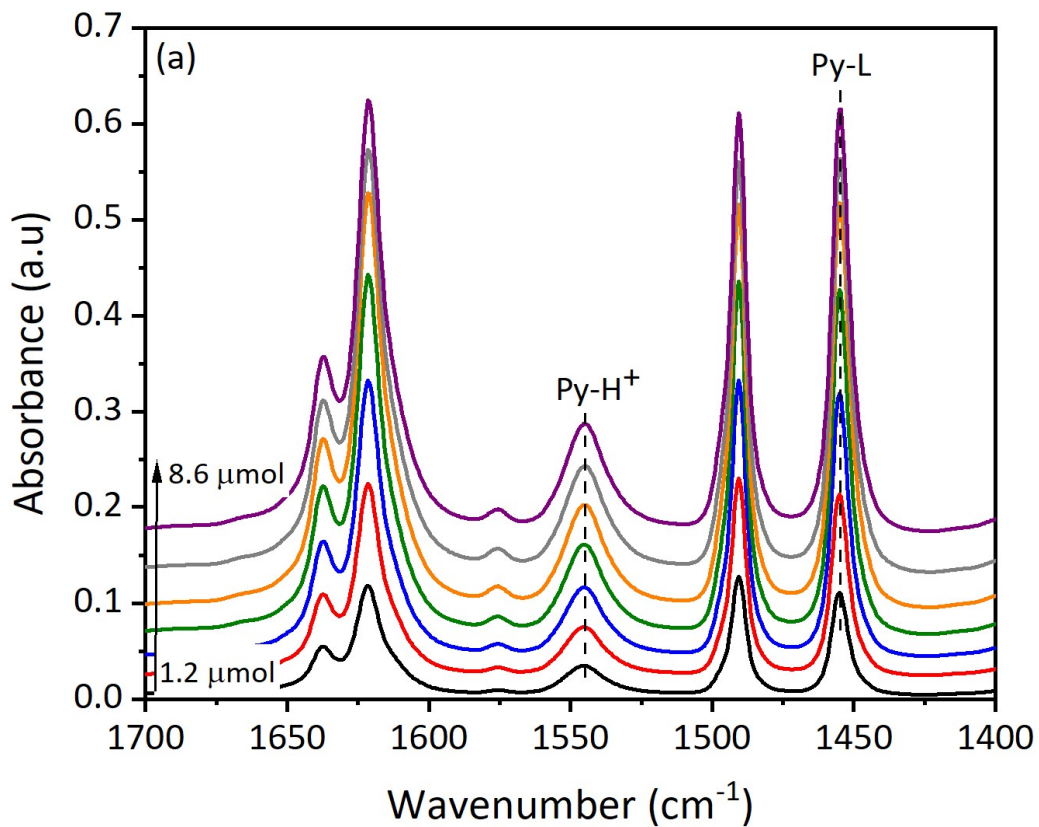
132 Following the traditional titration-style experiments (Figure 4), a linear relationship has been
133 obtained between the amount of Py introduced and the changes in the peak intensities, e.g. at ~ 1545
134 cm^{-1} for Py-B and at $\sim 1456\text{ cm}^{-1}$ for Py-L complexes following the first few injections. When all
135 sites are saturated, Py is no longer adsorbed on BAS and LAS, hence a plateau is observed and the
136 number of acid sites can be calculated from the titration graph. It should be noted that the amount of
137 Py interacting with acid sites is determined from the titration experiments with a degree of
138 uncertainty as some Py is likely to be adsorbed on the walls of the IR cell and the vacuum system.
139 The best way to minimise this uncertainty is to measure the mass of the sample during Py
140 adsorption-desorption and monitor its FTIR spectra at the same time in a single experiment, which
141 is achieved by the AGIR methodology.

142



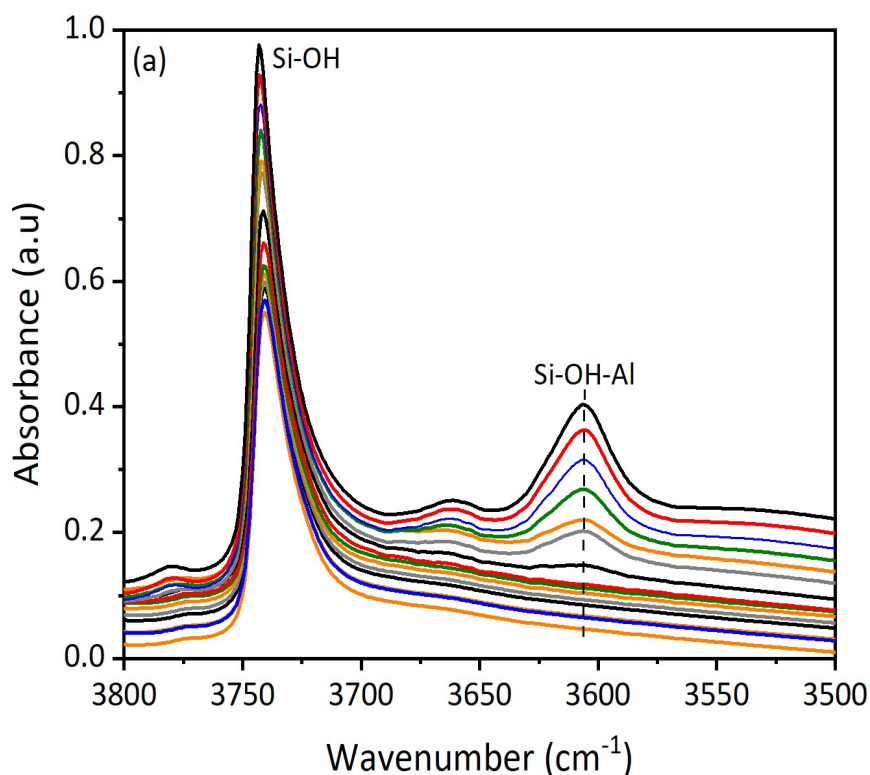
144 **Figure 3.** Linear relationship between the zeolite disc mass and the integrated absorbance of the IR
145 bands of (a) OH groups and (b) Py adsorbed on BAS and LAS in BEA-12 zeolite.

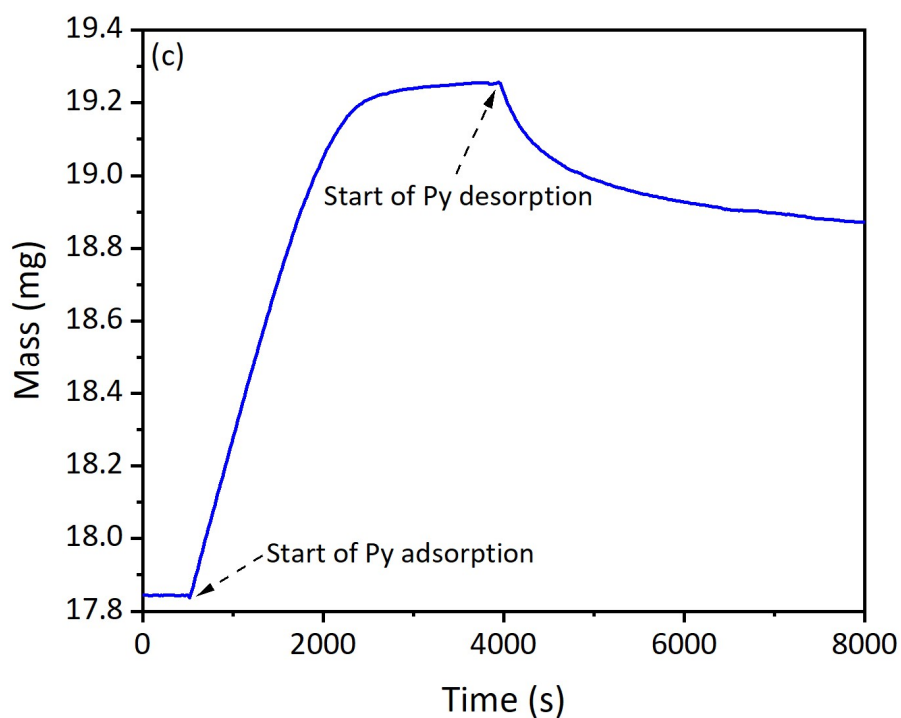
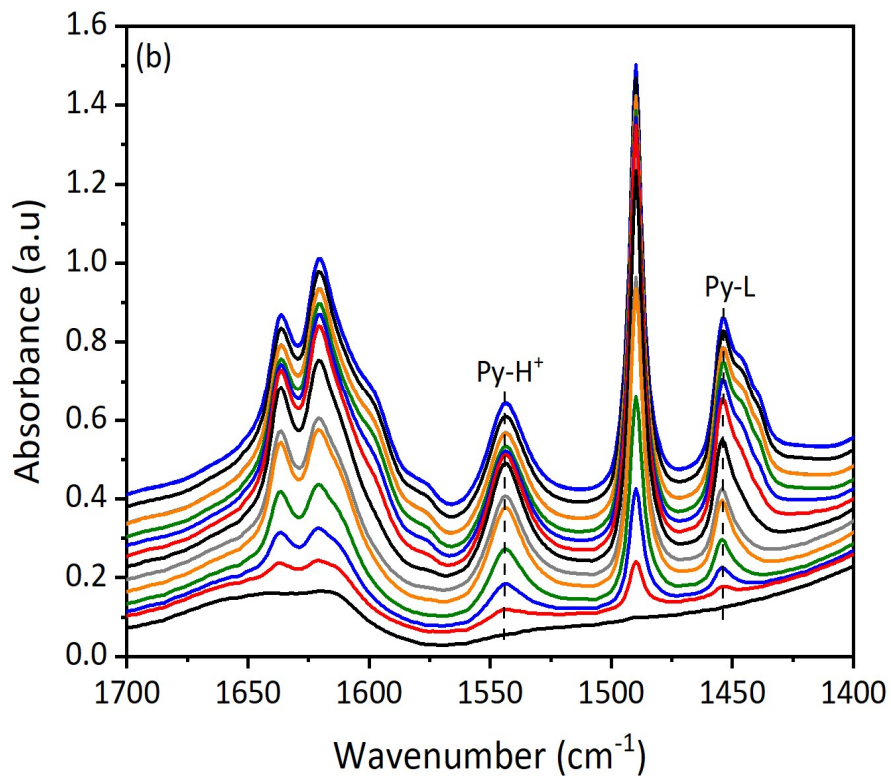
146



147 **Figure 4.** Zeolite BEA-12-600°C: titrations of BAS and LAS with Py at 150°C. (a) Difference FTIR
 148 spectra of the Py region. (b) Integrated peak area as a function of the increasing amount of added Py
 149 (spectra collected at 90°C).

150 Figure 5 presents an example of AGIR data collected following Py adsorption-desorption on a
151 sample of BEA-12. The integration of a microbalance and an infrared in situ flow-cell in a single
152 set-up affords simultaneous monitoring of the weight changes (TG signal) of the sample and the
153 spectra acquisition (FTIR signal). The temporal resolution of the TG analysis in this work is ~ 10
154 seconds and that for the FTIR measurements is ~ 30 seconds (both could be improved by a factor of
155 ~ 10 if required). As the accuracy of the mass measurements is better than $\pm 1 \mu\text{g}$ and a typical
156 amount of Py adsorbed is between 100 and 2000 μg per sample, highly accurate measurements of
157 the molar absorption coefficients of adsorbed Py species can be achieved from the combination of
158 the TG and FTIR data. In general, the spectroscopic data acquired using this methodology are in
159 agreement with the spectral observations obtained by in situ FTIR, that is Py adsorption at 150°C on
160 BEA-12 leads to the formation of peaks at ~ 1545 and $\sim 1455 \text{ cm}^{-1}$ corresponding to Py-B and Py-L
161 complexes (spectra of other zeolites before and after Py adsorption are provided in the Appendix of
162 the SI section). However, when the dynamic TG and FTIR signals are overlaid, they do not
163 coincide, showing a time lag of ~ 5 minutes (Figure S11), whereas the MS monitoring the
164 downstream concentration of Py confirms a typical break-through “chromatographic” behaviour of
165 the zeolite sample in the AGIR cell. Therefore, any quantitative kinetic type measurements in any
166 similar system, e.g. time-resolved diffusion or adsorption experiments, should be carried out with
167 great care. All the AGIR data utilised in this work for the calculation of $\epsilon(\text{Py-B})$ and $\epsilon(\text{Py-L})$ have
168 been obtained following Py desorption, rather than adsorption, allowing for the system equilibration
169 for at least 20 minutes.
170





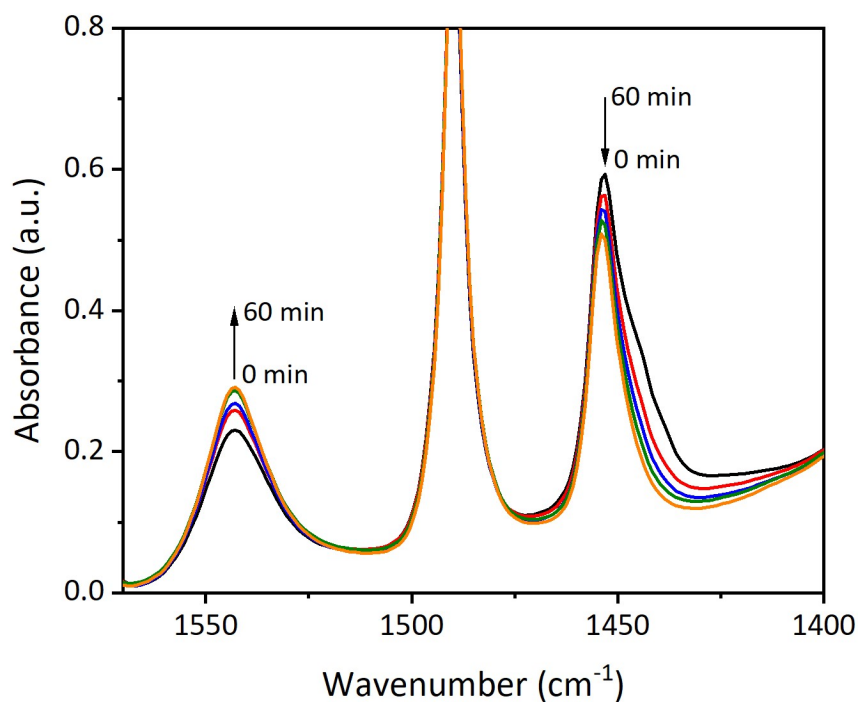
171 **Figure 5.** FTIR spectra of the (a) OH-region and (b) Py region following Py adsorption at 200°C on
 172 BEA-12 and (c) TGA data obtained on BEA-12 in the course of the AGIR experiment (data
 173 collected at 200°C).

174

175 Effect of physisorbed Py species.

176 Py adsorption on zeolites is typically performed at 30-150°C followed by the removal of
177 physisorbed Py species, which are held on the zeolite surface by weak hydrogen-bonding and van-
178 der-Waals interactions giving rise to the peaks at 1585-1595 and 1438-1445 cm⁻¹ [1,45]. The effect
179 of physisorbed Py on the intensity of the IR bands is exemplified by the spectra obtained for BEA-
180 12 zeolite after Py desorption at 200°C (Figure 6). Over ~60 minutes, the intensity of the peak
181 shoulder at ~1440 cm⁻¹ decreases, indicating that the physisorbed Py species are being removed at
182 200°C. At the same time, the TG signal shows a ~27% decrease (from 850 to 615 μmol/g), but the
183 intensity of the peak corresponding to Py-B species at ~1545 cm⁻¹ increases by ~25%. These
184 observations can be explained by a “solvent” effect, as weakly bound Py molecules reduce the
185 transient dipole moment of the protonated Py-H⁺ species (probably, by forming Py···Py-H⁺
186 complexes, in which the N-atom of the Py molecule forms a H-bond with the pyridinium ion) that
187 would cause a decrease in the value of ε(Py-B). Py is not the only basic test-molecule, for which
188 analogous “solvent” effect has been detected. Indeed, similar observations have been reported for
189 ammonia adsorption on H-forms of zeolites ZSM-5, BEA, MOR and Y with the formation of
190 [NH₄···NH₃]⁺ dimers and their subsequent solvation by excess ammonia [46]. Our data demonstrate
191 that the removal of physisorbed Py species should be conducted preferably at 200°C (150-200°C
192 depending on the zeolite) by purging or evacuation and should be monitored to ensure the one-to-
193 one interaction between Py and BAS, and hence, the accuracy of acidity measurements.

194



195

196 **Figure 6.** Difference FTIR spectra of Py adsorbed at 200°C on BEA-12 zeolite after desorption
197 over 60 min (spectra collected at 200°C; the arrows indicate an increase or decrease in the intensity
198 of IR peaks).

199

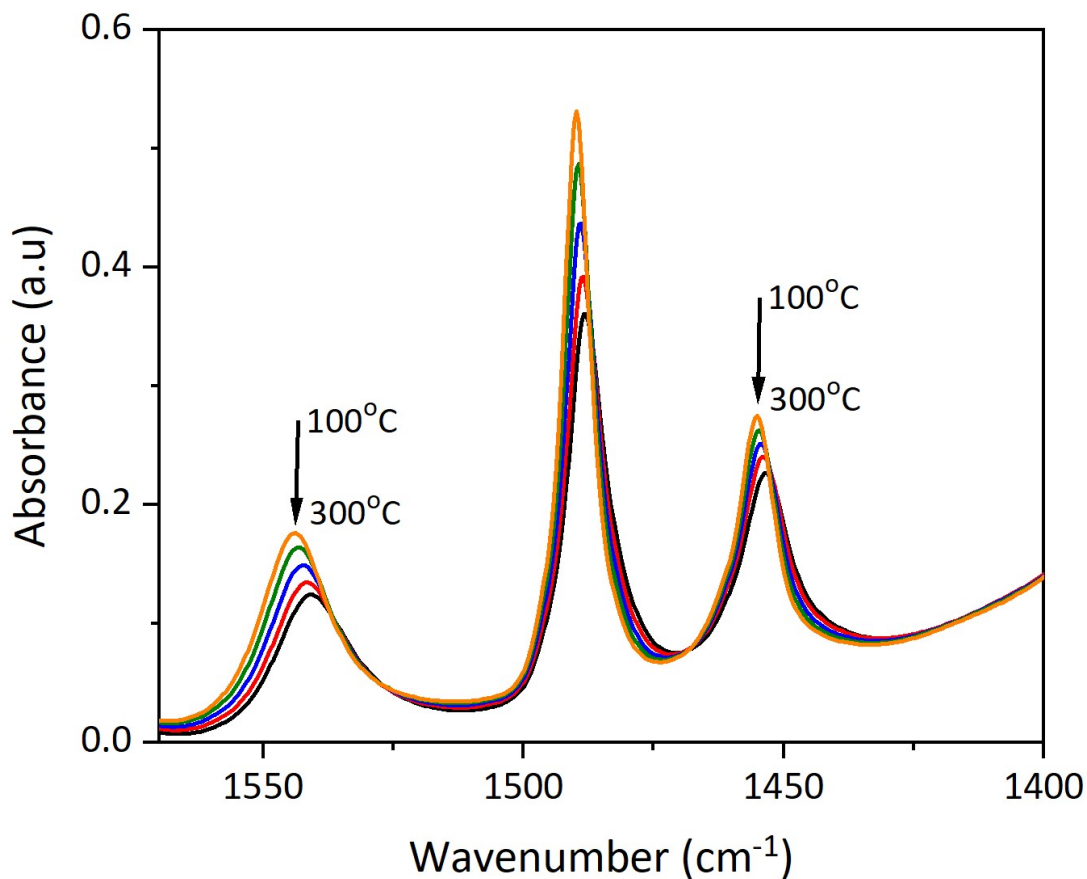
200 Effect of the spectral resolution.

201 The effect of resolutions on Py-B and Py-L peaks has been studied for BEA-19 following Py
202 adsorption at 150°C (Figure S12 and Table S2). Significant differences can be observed in the
203 shape and intensity of the Py-B, and particularly, the Py-L peaks. This can be attributed to the
204 greater width of the Py-B peak (FWHH~16 cm⁻¹) as compared to that for Py-L (FWHH~7 cm⁻¹).
205 The calculation of the peak intensities reveals noticeable potential experimental errors associated
206 with collecting the spectroscopic data at different resolutions, especially when the measurements
207 are done by the peak height (~17% for Py-L at 4 cm⁻¹ resolution, see Table S2). Table 1 shows
208 significant differences in the experimental approaches described in the literature, including the
209 resolution at which the IR spectra are obtained. A rather common resolution used is 4 cm⁻¹,
210 however, the values do vary, and frequently are not mentioned at all, which could be one of the
211 factors leading to discrepancies in the reported data. Clearly, it is best to compare the results
212 obtained under the same conditions, but if this is not possible, it is advisable to use calculations
213 based on peak area instead of peak height, or to apply correction values provided in Table S2.

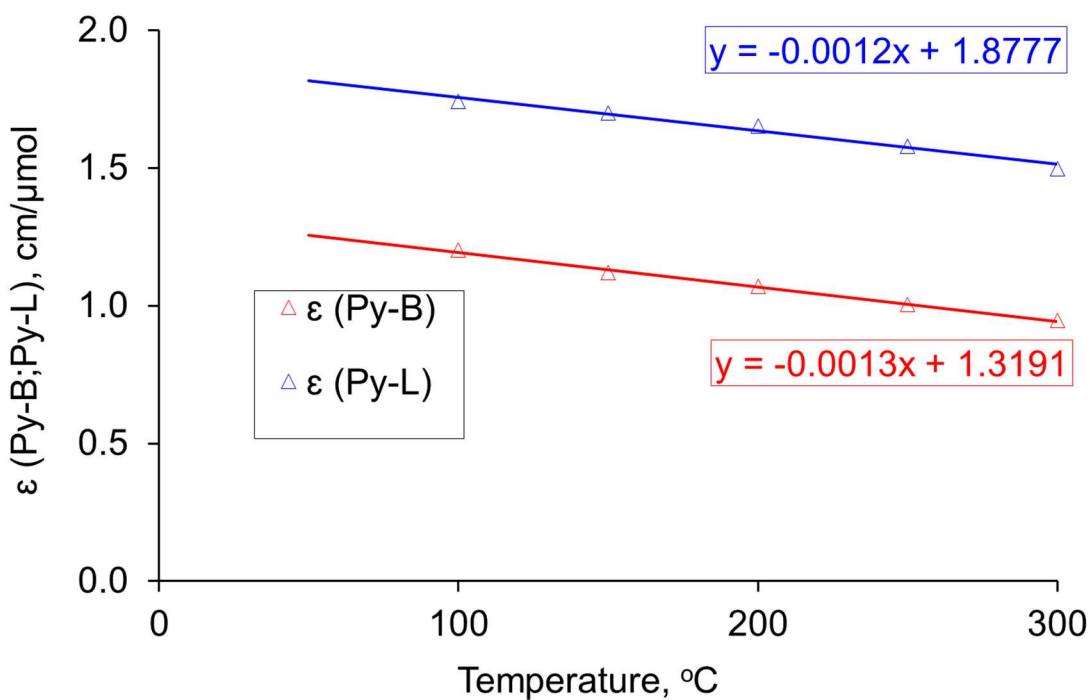
214 Effect of the temperature.

215 Our experimental data demonstrate that the temperature of the FTIR measurements has a
216 significant effect on the calculated ϵ values (Figure 7). With the increase in the temperature of the
217 sample under examination, both Py-B and Py-L bands are red-shifted, they become broader and
218 their intensity decreases (both the peak height and peak area). For instance, as the temperature of
219 the sample in the IR cell increases by 100°C, the Py-B peak shifts by ~2 cm⁻¹ and the Py-L peak
220 shifts by ~1 cm⁻¹ and their peak areas, and hence the measured value of the integrated molar
221 absorption coefficients, decrease by ~10% (the effect is reversible as the measurement temperature
222 is increased or decreased). The results, obtained for ZSM-5, BEA, FAU and MOR zeolites and
223 summarised in Figure S13 and Tables S3 and S4, provide clear experimental evidence that $\epsilon(\text{Py-B})$
224 and $\epsilon(\text{Py-L})$ values do depend on the temperature of the FTIR measurements, which disagrees with
225 previous assumptions [13,18]. Furthermore, as indicated in Table 1, the experimental temperature of
226 the data collection is not specified in many published reports, which can introduce yet another
227 source of uncertainty in the calculation of the number of acid sites in zeolite-based catalysts if
228 “random” literature data for the molar absorption coefficients are used. It should be noted that
229 similar effects are observed for the isolated OH-groups in all studied zeolites (both the red-shift and
230 a decrease in the peak area at higher temperatures). As the temperature of the FTIR measurements
231 is increased by 100°C, the Si-OH peak shifts by ~2 cm⁻¹ and peak of the bridging OH-groups shifts
232 by ~4 cm⁻¹, accompanied by a 10-15% decrease in the peak area (Table S4).

233



234
235



236

237 **Figure 7.** (a) FTIR spectra of Py adsorbed on BEA-12. Py was adsorbed at 150°C and then
 238 desorbed at 350°C; next, the sample temperature was decreased and the spectra collected at 100-
 239 300°C. (b) Molar absorption coefficients of Py-B and Py-L complexes for BEA-12 as a function of
 240 temperature of the FTIR measurements.

241 The modified Beer-Lambert-Bouguer law (Equation 1), which is commonly used in FTIR
 242 research on solid acid catalysts, allows the calculation of the ϵ values when the total amount of Py
 243 introduced and the intensity of the peak (Py-B or Py-L) are known.

$$A = \epsilon \frac{n^{Py}}{S} \quad (1)$$

244 where n^{Py} is the number of Py species (in μmol) in the sample disc, A is the peak area (in cm^{-1}) and
 245 S is the cross-section area of the zeolite disc ($S=1.3 \text{ cm}^2$ for in situ studies and $S=2.0 \text{ cm}^2$ for AGIR
 246 experiments). For each material under investigation, the integrated areas of the peaks corresponding
 247 to Py adsorbed on BAS and LAS and n^{Py} values (obtained from the TG signal and utilised to
 248 determine the number of BAS and LAS, Table 3) have been used to calculate $\epsilon(\text{Py-B})$ and $\epsilon(\text{Py-L})$
 249 according to Equation 1 using a number of repeat experiments. The data obtained at different
 250 temperatures for zeolites ZSM-5, BEA, MOR and FAU are summarised in Tables 2 and S3 and
 251 Figure S13. An important conclusion, which can be drawn from these data, is that the $\epsilon(\text{Py-B})$
 252 values are dependent on the zeolite structure, whilst the $\epsilon(\text{Py-L})$ values are very similar even for
 253 different types of LAS.
 254

255
 256 **Table 2.** Values of the integrated molar absorption coefficients for Py-B and Py-L complexes on
 257 various zeolites determined from the AGIR and in situ experiments.

Sample	ϵ (Py-B)*, $\text{cm}/\mu\text{mol}$			ϵ (Py-L)*, $\text{cm}/\mu\text{mol}$		
	30°C	150°C	200°C	30°C	150°C	200°C
$\gamma\text{-Al}_2\text{O}_3$				1.87±0.1	1.71±0.1	1.65±0.1
ZSM-5 Si/Al=27-40	1.23±0.08	1.09±0.08	1.05±0.08			
BEA Si/Al=12-19	1.26±0.16	1.12±0.16	1.07±0.15			
MOR Si/Al=10	1.38±0.04	1.29±0.04	1.23±0.04			
FAU Si/Al=2.6	1.65±0.15	1.54±0.15	1.46±0.15			
CaZSM-5 Si/Al=40				1.87±0.2	1.71±0.2	1.64±0.2
NaZSM-5 Si/Al=40				1.88±0.2	1.72±0.2	1.65±0.2

258 * $\epsilon(\text{Py-B})$ and $\epsilon(\text{Py-L})$ data reported for 200°C are experimental AGIR values and those for
 259 30°C and 150°C are obtained by extrapolation and verified using in situ experiments.
 260

261 **Table 3.** The number of BAS and LAS obtained for the studied zeolites from AGIR experiments.

Sample	BAS, $\mu\text{mol/g}$	LAS, $\mu\text{mol/g}$
$\gamma\text{-Al}_2\text{O}_3$	-	125
ZSM-5-40	325	10
ZSM-5-27	450	10
BEA-12	495	120
BEA-19	485	65
MOR-10	970	5
FAU-C	1080	20

262 * BAS and LAS data reported are experimental AGIR values obtained following Py
 263 desorption at 200°C. Not all acid sites are accessible in MOR and FAU zeolites.
 264

265 Analysis of the experimental data for the samples containing both BAS and LAS.

266 As zeolites often have both BAS and LAS, the relationship between the amount of Py
 267 interacting with acid sites and the molar absorption coefficient values is given by the following
 268 equations:

269
$$n_{total}^{Py} = n_B^{Py} + n_L^{Py} \quad \text{or} \quad (2)$$

270
$$n_{total}^{Py} = \frac{A_B \times S}{\epsilon_B} + \frac{A_L \times S}{\epsilon_L} \quad (3)$$

271 Equation 3 contains two unknown parameters (ϵ_B and ϵ_L , these stand for $\epsilon(\text{Py-B})$ and $\epsilon(\text{Py-L})$)
 272 and in a single experiment it is not possible to determine both of them. Therefore, it is necessary to
 273 use zeolites with different BAS/LAS ratios (zeolites calcined at four different temperatures have
 274 been used in this work). Then, the calculation of both ϵ_{BAS} and ϵ_{LAS} can be achieved by applying a
 275 linearised form of Equation 3 shown below.

276
$$\frac{A_B \times S}{n_{total}} = -\frac{\epsilon_B}{\epsilon_L} \times \frac{A_L \times S}{n_{total}} + \epsilon_B \quad (4)$$

277 Using Equation 4, both $\epsilon(\text{Py-B})$ and $\epsilon(\text{Py-L})$ values can be determined from the slope and
 278 the y-intercept of the trend line. Indeed, a similar approach has been suggested previously [18,39]
 279 based on the assumption that $\epsilon(\text{Py-B})$, as well as $\epsilon(\text{Py-L})$ values, are the same for different solid
 280 acid catalysts. Although both $\epsilon(\text{Py-B})$ and $\epsilon(\text{Py-L})$ can be calculated from FTIR *in situ* experiments,
 281 our data presented in Tables 2 and S3 and Figures S13 and S14 clearly demonstrate that the $\epsilon(\text{Py-B})$
 282 values are dependent on the zeolite structure, which contradicts the earlier conjecture made in the

283 literature [18,39]. In addition, this approach leads to a significant variation in calculated values of
284 the molar absorption coefficients, particularly for the Py-L complexes. This is related to the fact that
285 the accuracy of the suggested model is strongly dependent on the experimental parameters. Firstly,
286 from the results presented in Figure S14, it is self-evident that if data for different zeolites are
287 grouped together, then the “mean” values of $\epsilon(\text{Py-B})$ and $\epsilon(\text{Py-L})$ would be determined by the
288 choice of the selected or available experimental data points, and hence, would be different for
289 different investigations, if the data for different zeolite types are indeed combined in such
290 investigations. Secondly, an important limitation of this model is the potentially inaccurate value of
291 the total amount of Py chemisorbed on the zeolite disc. As mentioned previously, an unknown
292 quantity of Py can be adsorbed on the walls of the IR cell leading to the erroneous determination of
293 the amount of the probe molecule interacting with each type of acid sites, which would strongly
294 affect the calculations [40,47]. (It should be noted that the application of AGIR methodology in this
295 work virtually eliminates this problem.) Thirdly, the principal assumption of this model is that only
296 one type of BAS and one type of LAS are present within the zeolite structures. However, in
297 practice, this is not true in most cases. For instance, a significant number of defect sites are present
298 in zeolite BEA, such as Si-OH and Al-OH groups with weak or moderately strong Brønsted acidity,
299 while the nature of Lewis acidity is still under discussion. Hence, the molar absorption coefficient
300 values presented in Table S5 show particularly poor statistics for zeolite BEA, even though the first
301 two limitations of this model have been minimised in this work. For all these reasons, the
302 quantitative evaluation of acidity in solid catalysts containing a range of both BAS and LAS may be
303 associated with significant errors and should be carried out with a great deal of care.

304 Practical recommendations.

305 The following suggestions, aiming to enhance the quality of FTIR characterisation of acid
306 sites in zeolites and to ensure its quantitative nature, can be made.

307 For the preparation of the self-supported disks, the amount of the sample should be kept
308 between 5 and 15 mg per cm^2 and preferably no higher than 10 mg per cm^2 , to ensure both good
309 signal to noise ratio and linearity between absorbance and surface concentration.

310 The load applied when pressing the samples should not exceed 0.5 tonne per cm^2 in order to
311 avoid possible incomplete activation and structural degradation of the zeolite. The design of the IR
312 cell for kinetic type measurements and other experimental parameters, e.g. the activation
313 temperature and the number of repeat samples, should be carefully considered and tested.

314 Physisorbed Py should be removed, its evacuation should be conducted preferably at 200°C
315 and should be monitored spectroscopically. The desired spectral resolution should be chosen with
316 care (the commonly used resolution of 4 cm^{-1} is recommended), and the intensity of infrared bands
317 of Py-L and Py-B complexes should be measured as peak area, rather than peak height.

318 The effects of the sample temperature on the measurements of the position and intensity of
319 infrared bands ($\sim 10\%$ decrease per 100°C difference) should be taken into account to enable a
320 quantitative comparison with the literature data. As the values of $\epsilon(\text{Py-B})$ are affected by the zeolite
321 structure and composition, additional calibration and cross-correlation with other analytical
322 techniques may be required, especially for solids containing both BAS and LAS. In general, such
323 calibrations should be performed separately for different types of zeolites.

324 Finally, we suggest that a systematic indication of the following elements in experimental
325 reports would be a good practice: (i) amount of zeolite per unit disc area (e.g. 10 mg cm^{-2}), (ii)
326 pressure applied for the preparation of the disc (e.g. 0.5 tonne cm^{-2}), (iii) conditions of activation of
327 the sample prior adsorption (e.g. under vacuum at 450°C for 5 hours), (iv) conditions of pyridine
328 adsorption (e.g. 150°C , 0.5 mbar equilibrium pressure), (v) precautions taken to remove
329 physisorbed species (e.g. evacuation at 200°C), (vi) spectral resolution (e.g. 4 cm^{-1}), (vii) sample
330 temperature during the acquisition of spectra (e.g. 30°C).

331

332 5. Conclusions

333 This study presents a detailed methodology for accurate calculation of the integrated molar
334 absorption coefficients of Py complexes, $\epsilon(\text{Py-B})$ and $\epsilon(\text{Py-L})$, which are essential for quantitative
335 characterisation of the acidic properties of zeolites. This work demonstrates that the Beer-Lambert-
336 Bouguer law is valid for IR characterisation of zeolites and makes it evident that careful design of
337 the experimental procedures is essential for quantitative FTIR measurements. The obtained values
338 of the molar absorption coefficients presented here can be used directly to determine the number of
339 acid sites in different zeolites if the experimental conditions match those utilised in our work. If the
340 conditions are different, then the correlations and detailed quantitative data provided in this paper
341 and in Supporting Information should be sufficient to make the necessary adjustments.

342 The direct quantitative measurements of the molar absorption coefficients using AGIR
343 experiments demonstrate that the values of $\epsilon(\text{Py-B})$ depend on the zeolite structure, increasing in the
344 order $\text{ZSM-5} \approx \text{BEA} < \text{MOR} < \text{FAU}$, which could be linked to the changes in Si/Al ratio, the acid
345 site strength and confinement effects, all of which can alter the localised electrostatic field around
346 adsorbed Py species, thus affecting the magnitude of the transient dipole moment of protonated Py
347 that governs the value of $\epsilon(\text{Py-B})$. In contrast, the transient dipole moment of Py molecules
348 coordinated to LAS (rather than protonated) appears to be influenced significantly less. Indeed, the
349 $\epsilon(\text{Py-L})$ values are almost the same, within the error of the measurements, for different zeolite
350 structures and even for Py interacting with Na^+ and Ca^{2+} cations. Additionally, a clear correlation is
351 established between the temperature of the infrared measurements and the magnitude of the molar
352 absorption coefficients, which decrease by $\sim 10\%$ as the temperature increases by 100°C , and a
353 similar effect is observed for other vibrating species. The unusual attenuation of the intensity of Py-

354 B peak by physisorbed Py, which apparently reduces the value of $\epsilon(\text{Py-B})$, has been clearly
355 identified. Likewise, the effects of the experimental methodology, e.g. the spectral resolution, have
356 been evaluated and quantified.

357 Although quantum chemical calculations have not been planned as part of this research, it is
358 clear that with the achieved quality of the experimental data there is a scope for computational
359 modelling of the effects of the Si/Al ratio, confinement in micropores, the nature of acid sites,
360 adsorption temperatures and physisorbed species on the magnitude of the transient dipole moment
361 of various species present in zeolites. The experimental work can be also extended to the evaluation
362 of other solid acids and catalytic materials containing different types of BAS and LAS as well as to
363 the investigation of the effects of acid site strength and of the zeolite structure on the values of ϵ .
364 The experimental $\epsilon(\text{Py-B})$ and $\epsilon(\text{Py-L})$ values obtained should significantly improve the accuracy of
365 the quantitative analysis of acidic properties of zeolite-based catalysts using IR spectroscopy.

366

367 **Acknowledgments**

368 The authors thank ENSICAEN for the overall support for this research programme. We
369 gratefully acknowledge Johnson Matthey PLC and Keele University (ACORN-2015 grant) for their
370 support and funding provided for this work as the PhD studentship for C.F. M.J. thanks Keele
371 University (ACORN-2018 grant), the Royal Society (International Exchanges grant IE160562) and
372 the Newton Fund (Institutional Links grant 261867079) for supporting his PhD project. The authors
373 thank Dr. D. Broom for providing a sample of NIST reference material RM8852, Prof. A.Y.
374 Khodakov for providing a sample of alumina and Dr. A. Vicente for assistance with the MAS NMR
375 measurements.

376

377 **Supplementary Information**

378 Supplementary data for this article can be found on-line at:

379

380 **Conflict of interest.**

381 The authors declare no competing financial interest.

382

383 **References**

- [1] K. Hadjiivanov. *Identification and characterization of surface hydroxyl groups by infrared spectroscopy*. Adv. Catal., 2014, 57, 99-318.
- [2] C. Morterra, G. Magnacca, V. Bolis. *On the critical use of molar absorption coefficients for adsorbed species: the methanol/silica system*. Catal. Today, 2001, 70, 43–58

- [3] N.S. Nesterenko, F. Thibault-Starzyk, V. Montouillout, V. V. Yushchenko, C. Fernandez, J.P. Gilson, F. Fajula, I.I. Ivanova. *The use of the consecutive adsorption of pyridine bases and carbon monoxide in the IR spectroscopic study of the accessibility of acid sites in microporous/mesoporous materials*. Kinet. Katal., 2006, 47 (1), 40-48.
- [4] K. Góra-Marek, K. Tarach, M. Choi. *2,6-di-tert-butylpyridine sorption approach to quantify the external acidity in hierarchical zeolites*. J. Phys. Chem. C, 2014, 118, (23), 12266-12274.
- [5] T. Onfroy, G. Clet, M. Houalla. *Quantitative IR characterization of the acidity of various oxide catalysts*. Micro. Meso. Mater., 2005, 82, (1-2), 99-104.
- [6] B. Wichterlová, Z. Tvarukzová, Z. Sobalík, P. Sarv. *Determination and properties of acid sites in H-ferrierite. A comparison of ferrierite and MFI structures*. Micro. Meso. Mater., 1998, 24, 223-233.
- [7] P. Bazin, A. Alenda, F. Thibault-Starzyk. *Interaction of water and ammonium in NaHY zeolite as detected by combined IR and gravimetric analysis (AGIR)*. Dalton Trans., 2010, 39 (36), 8432-8436.
- [8] A.A. Gabrienko, I.G. Danilova, S.S. Arzumanov, L.V. Pirutko, D. Freude, A.G. Stepanov. *Direct Measurement of Zeolite Brønsted Acidity by FTIR Spectroscopy: Solid-State ¹H MAS NMR Approach for Reliable Determination of the Integrated Molar Absorption Coefficients*. Phys. Chem. C, 2018, 122, 25386-25395.
- [9] M. R. Basila, T. R. Kantner, K. H. Rhee. *The nature of the acidic sites on a silica-alumina. Characterization by infrared spectroscopic studies of trimethylamine and pyridine chemisorption*. J. Phys. Chem., 1964, 68 (11), 3197-3207.
- [10] M. R. Basila, T. R. Kantner. *The nature of the acidic sites on silica-alumina. A reevaluation of the relative absorption coefficients of chemisorbed pyridine*. J. Phys. Chem., 1966, 70 (6) 1681-1682.
- [11] T. R. Hughes, H. M. White. *Study of the surface structure of decationized Y zeolite by quantitative infrared spectroscopy*. J. Phys. Chem., 1967, 71 (7), 2192-2201.
- [12] F. R. Cannings. *Acidic sites on mordenite. An infrared study of adsorbed pyridine*. J. Phys. Chem., 1968, 72 (13) 4691-4693.
- [13] M. Lefrancois, G. Malbois. *The nature of the acidic sites on mordenite. Characterization of adsorbed pyridine and water by infrared study*. J. Catal., 1971, 20, 350-358.
- [14] J. Datka. *Transformations of but-1-ene molecules adsorbed in NaHY zeolites studied by infrared spectroscopy*. J.C.S Faraday I., 1980, 76, 2437-2447.
- [15] J. Datka. *Dehydroxylation of NaHY zeolites studied by infrared spectroscopy*. J. Chem. Soc., Faraday Trans., 1, 1981, 77, 2877-2881.
- [16] J. Take, T. Yamaguchi, K. Miyamoto, H. Ohyama, M. Misono, *Brønsted site population on external and on internal surface of shape-selective catalysts*. Stud. Surf. Sci. Catal., 1986, 28, 495-502.
- [17] J. Datka, A. M. Turek, J.M. Jehng, I. E. Wachs. *Acidic properties of supported niobium oxide catalysts: An infrared spectroscopy investigation*. J. Catal., 1992, 135 (1), 186-199.

- [18] C. A. Emeis. *Determination of integrated molar extinction coefficients for infrared absorption bands of pyridine adsorbed on solid acid catalysts*. J. Catal., 1993, 141 (2), 347-354.
- [19] I. Kiricsi, C. Flego, G. Pazzuconi, W. O. Parker, Jr., R. Millini, C. Perego, G. Bellussi. *Progress toward understanding zeolite β acidity: An IR and ^{27}Al NMR spectroscopic study*. J. Phys. Chem., 1994, 98, 4627-463.
- [20] S. Khabtou, T. Chevreau, J. C. Lavalley. *Quantitative infrared study of the distinct acidic hydroxyl groups contained in modified Y zeolites*. Microporous Mater., 1994, 3, 133-148.
- [21] M. A. Makarova, K. Karim, J. Dwyer. *Limitation in the application of pyridine for quantitative studies of Brønsted acidity in relatively aluminous zeolites*. Microporous Mater., 1995, 4, 243-246.
- [22] M. Maache, A. Janin, J.C. Lavalley, E. Benazzi. *FT infrared study of Brønsted acidity of H-mordenites: heterogeneity and effect of dealumination*. Zeolites., 1995, 15, 507-516.
- [23] J. Datka, B. Gil, A. Kubacka. *Heterogeneity of OH groups in H-mordenites: Effect of dehydroxylation*. Zeolites., 1996, 17, 428-433.
- [24] M. Guisnet, P. Ayrault, C. Coutanceau, M. F. Alvarez, J. Datka. *Acid properties of dealuminated beta zeolites studied by IR spectroscopy*. J. Chem. Soc., Faraday Tran., 1997, 93 (8), 1661-1665.
- [25] B. Sulikowski, J. Datka, B. Gil, J. Ptaszynski, J. Klinowski. *Acidity and catalytic properties of realuminated zeolite Y*. J. Phys. Chem. B, 1997, 101, 6929-6932.
- [26] M. Guiset, P. Ayrault, J. Datka, *Acid properties of mazzite zeolites studied by IR spectroscopy*. Micro. Meso. Mater., 1998, 20, 283-291.
- [27] A. Taouli, A. Klemm, M. Breede, W. Reschetilowski. *Acidity investigations and determination of integrated molar extinction coefficients for infrared adsorption bands of ammonia adsorbed on acidic sites of MCM-41*. Stud. Surf. Sci. Catal., 1999, 125, 307-314.
- [28] E. Selli, L. Forni. *Comparison between the surface acidity of solid catalysts determined by TPD and FTIR analysis of pre-adsorbed pyridine*. Micro. Meso. Mater., 1999, 31, 129-140.
- [29] F. Thibault-Starzyk, B. Gil, S. Aiello, T. Chevreau, J. P. Gilson. *In situ thermogravimetry in an infrared spectrometer: an answer to quantitative spectroscopy of adsorbed species on heterogeneous catalysts*. Micro. Meso. Mater., 2004, 67, 107-112.
- [30] K. Góra-Marek, M. Derewinski, P. Sarv, J. Datka. *IR and NMR studies of mesoporous alumina and related aluminosilicates*. Catal. Today, 2005, 101, 131-138.
- [31] K. Góra-Marek, J. Datka, S. Dzwigaj, M. Che. *Influence of V content on the nature and strength of acidic sites in VSi β zeolite evidenced by IR spectroscopy*. J. Phys. Chem. B., 2006, 110, 6763-6767.
- [32] B. Gil, G. Kosová, J. Cejka, *Acidity of MCM-58 and MCM-68 zeolites in comparison with some other 12-ring zeolites*. Micro. Meso. Mater., 2010, 129, 256-266.
- [33] I. S. Pieta, M. Ishaq, R. P. K. Wells, J. A. Anderson. *Quantitative determination of acid sites on silica–alumina*. Appl. Catal. A., 390 (2010) 127–134.
- [34] J. M. R. Gallo, C. Bisio, G. Gatti, L. Marchese, H. O. Pastore. *Physicochemical characterization and surface acid properties of mesoporous [Al]-SBA-15 obtained by direct synthesis*. Langmuir., 2010, 26 (8), 5791–5800.

- [35] E. J. M Hensen, D. G. Poduval, V. Degirmenci, D. A. J. M, Ligthart, W. Chen, F. Maugé, M. S. Rigutto, J. A Rob van Veen. *Acidity characterization of amorphous silica–alumina*. J. Phys. Chem. C., 2012, 116, 21416-21429.
- [36] J. W. Harris, M. J. Cordon, J. R. Di Iorio, J. C. Vega-Vila, F. H. Ribeiro, R. Gounder. *Titration and quantification of open and closed Lewis acid sites in Sn-Beta zeolites that catalyze glucose isomerization*. J. Catal., 2016, 335, 141-154.
- [37] I. Miletto, G. Paul, S. Chapman, G. Gatti, L. Marchese, R. Raja, E. Gianotti, *Chem. Eur. J.*, 2017, 23, 9952-9961.
- [38] K. A. Tarach, K. Góra-Marek, J. Martinez-Triguero, I. Melián-Cabrera, *Acidity and accessibility studies of desilicated ZSM-5 zeolites in terms of their effectiveness as catalysts in acid-catalyzed cracking processes*. Catal. Sci. Technol., 2017, 7, 858-873.
- [39] N. S. Gould, B. Xu. *Quantification of acid site densities on zeolites in the presence of solvents via determination of extinction coefficients of adsorbed pyridine*. J. Catal., 2018, 358, 80-88.
- [40] S. Bordiga, C. Lamberti, F. Bonino, A. Travert, F. Thibault-Starzyk. *Probing zeolites by vibrational spectroscopies*. Chem. Soc. Rev., 2015. 44 (20): 7262-7341.
- [41] P. Stelmachowski, S. Sirotin, P. Bazin, F. Maugé, A. Travert, *Speciation of adsorbed CO₂ on metal oxides by a new 2-dimensional approach: 2D infrared inversion spectroscopy (2D IRIS)*. Phys. Chem. Chem. Phys. 2013, 15, 9335–9342.
- [42] B. Moulin, L. Oliviero, P. Bazin, M. Daturi, G. Costentin, F. Maugé, *How to determine IR molar absorption coefficients of co-adsorbed species? Application to methanol adsorption for quantification of MgO basic sites*. Phys. Chem. Chem. Phys. 2011,13, 10797–10807.
- [43] F. Vilmin, P. Bazin, F. Thibault-Starzyk, A. Travert, *Speciation of adsorbates on surface of solids by infrared spectroscopy and chemometrics* *Analytica Chimica Acta*. 2015, 891, 79-89.
- [44] S. Turner, J.R. Sieber, T.W. Vetter, R. Zeisler, A.F. Marlow, M.G. Moreno-Ramirez, M.E. Davis, G.J. Kennedy, W.G. Borghard, S. Yang, A. Navrotsky, B.H. Toby, J.F. Kelly, R.A. Fletcher, E.S. Windsor, J.R. Verkouteren, S.D. Leigh, *Characterization of chemical properties, unit cell parameters and particle size distribution of three zeolite reference materials: RM 8850 - zeolite Y, RM 8851 - zeolite A and RM 8852 - ammonium ZSM-5 zeolite*, Micro. Meso. Mater., 2008, 107, 252-267.
- [45] L. M. Parker, D. M. Bibby, G. R. Burns. *Fourier-transform infrared study of pyridine sorbed on zeolite HY*. J. Chem. Soc. Faraday Trans., 1991, 87 (19), 3319-3323.
- [46] A. Zecchina, L. Marchese, S. Bordiga, C. Paze, E. Gianotti. *Vibrational spectroscopy of NH₄⁺ ions in zeolitic materials: an IR study*. J. Phys. Chem. B, 1997, 101, 6929-6932.

[47] A. Popov, E. Kondratieva, J. M. Goupil, L. Mariey, P. Bazin J.-P. Gilson, A. Travert, F. Maugé. *Bio-oils hydrodeoxygenation: Adsorption of phenolic molecules on oxidic catalyst supports*. J. Phys. Chem. C., 2010, 114, 15661- 15670.